INTERNATIONAL INSTITUTE OF WELDING
A world of joining experience

Delegation of Austria, Sweden and Germany

XIII-2583-15

Crack propagation analysis and rehabilitation by HFMI of pre-fatigued welded structures

M. Leitner[1], Z. Barsoum[2] and F. Schäfers[3]

[1]Montanuniversität Leoben, Department Product Engineering, Chair of Mechanical Engineering, Austria

[2]KTH-Royal Institute of Technology, Department of Aeronautical and Vehicle Engineering, Division of Lightweight Structures, Sweden

[3]Pitec GmbH, Germany

Abstract

This paper deals with a crack propagation analysis of welded structures and rehabilitation after pre-fatigue loading by the high-frequency mechanical impact (HFMI) post-treatment technique. The investigated specimen type is a thin-walled longitudinal stiffener made of mild construction steel *S355*. Fatigue tests are performed for the as-welded and HFMI-treated condition with and without pre-cycling. Accompanying strain gauge measurements, optical surface crack detection, and micrographs enable fatigue testing up to a defined crack length of *a=1 mm*, which was set as initial condition for the rehabilitation step by the HFMI-treatment. Fracture mechanical calculations are primarily performed on the basis of the weight-function approach. Thereby, the local residual stress condition at the weld toe is considered by the aid of a structural weld simulation, whereat the numerically evaluated residual stress distribution in depth agrees well to X-ray measurement results. Additional numerical and analytical studies involving the influence of different weld toe radii and initial crack lengths are performed, which proof the basic applicability of the proposed values given in the IIW-recommendation. A comparison of the calculated lifetime values to the fatigue test results shows, that the weight-function approach matches the fatigue life well, but on contrary the standard fracture mechanical method based on parametric stress intensity equations leads to a significant conservative fatigue assessment. By application of the HFMI-treatment as rehabilitation method it is found that the beneficial post-treatment effect increases especially with a decreasing of the applied load-level. Hence, particularly for minor nominal stress ranges near the high-cycle fatigue region, the mechanical post-treatment as repair method is utmost effective leading to almost equal fatigue strength as for the HFMI-treated specimens without pre-cycling for the analysed crack size. Finally, proposals for the crack growth assessment of welded structures and a conservative application of HFMI as rehabilitation method for mild steel joints are provided.

Keywords: Fatigue strength, Crack propagation analysis, Weight-function approach, High frequency mechanical impact (HFMI) treatment, Rehabilitation of welded structures, Structural weld simulation

1 Introduction

To assess the fatigue strength of welded joints recommendations [1] are available, which involve different stress-based approaches, such as the nominal, the structural and the effective notch stress method. However, it is well known that the fatigue strength of welded parts is significantly affected by local properties, such as the local geometry at the weld toe or root and the residual stress condition. In addition, discontinuities like flaws, undercuts, or pores cannot be avoided during gas-metal arc welding and need to be statistically considered in the fatigue assessment, whereat fracture mechanical procedures based on an evaluation of the linear-elastic crack propagation are well suited for this kind of task [2, 3]. An important application area of this concept occurs in case of huge structures where it is mainly not possible to rebuild the whole structure after achieving the calculated lifetime and therefore, inspection intervals during the operation time need to be defined. If a crack is then non-destructively detected [4], different kinds of post-treatment techniques are feasible, at which one efficient method is offered by the high-frequency mechanical impact (HFMI) treatment. Recently, numerous investigations [5, 6] showed the beneficial effect of this method for an application without any cyclic pre-loading, but however, the application as rehabilitation purpose is not sufficient investigated yet.

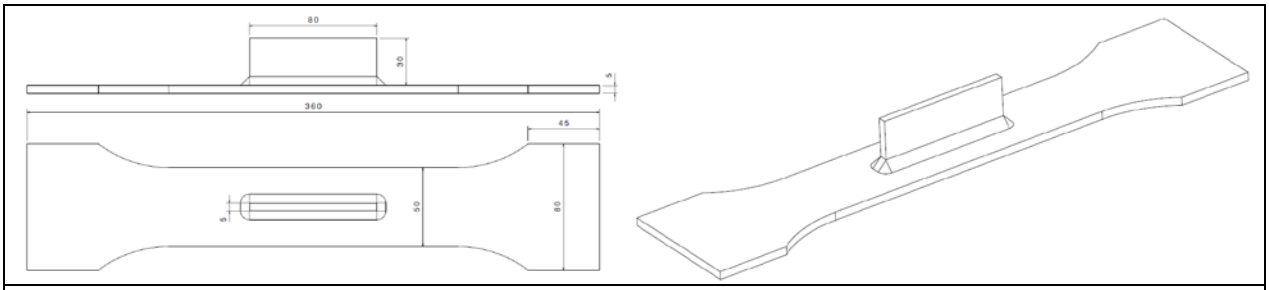

Figure 1: Geometry of investigated longitudinal stiffener specimen

Therefore, this paper contributes to the crack propagation analysis of welded joints and the subsequent rehabilitation of pre-fatigued structures by the HFMI post-treatment. As the fatigue crack growth regime is pre-dominant in case of notched joints, a longitudinal stiffener specimen made of mild steel *S355* is investigated, see Fig. 1.

2 Fatigue tests

At first, fatigue tests in the as-welded and HFMI-treated condition without any pre-fatigue of the specimens are performed. The stress ratio is set to *R=0.1* and the abort criterion is burst fracture. The evaluated nominal S/N-curves are presented in Fig. 2 exhibiting a survival probability of P_S=*97.7 %*.

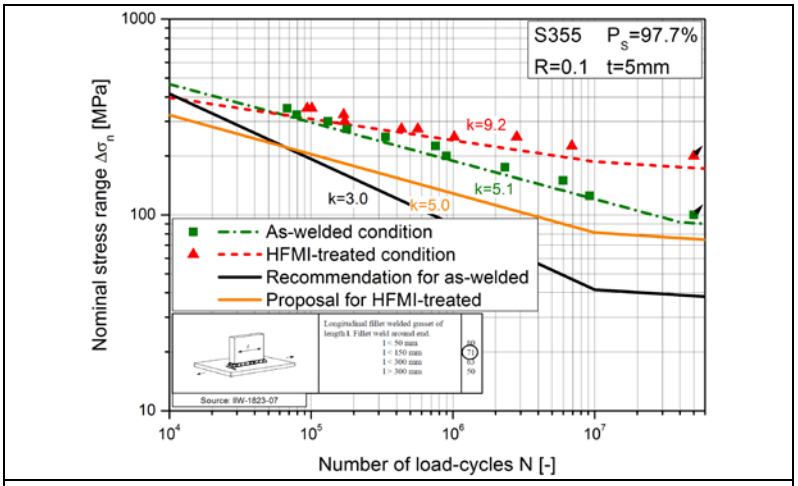

Figure 2: Nominal S/N-curves for as-welded and HFMI-treated condition

The results show, that the HFMI-treatment increases the fatigue strength especially in the high-cycle fatigue region due to a shift of the transition knee point to a lower lifetime. The nominal stress values of the HFMI-treated specimens at the run-out level at fifty million load-cycles exceed with $\Delta\sigma_n$=200MPa the as-welded condition by a factor of two. In the finite lifetime regime an improvement is still observable, mainly due to an increase of the slope from *k=5.1* for the as-welded to *k=9.2* for the post-treated specimens. A comparison to the recommended [1] curve for the as-welded and the proposed [7] curve for the HFMI-treated condition indicates a high welding and post-treatment quality which fulfil the recommended demands [8].
For an analysis of the technical crack initiation and the subsequent macroscopic crack propagation, strain gauges at the weld toe region of the end-of-seam areas are applied and optical measurements by the aid of a zinc-oxide paste as contrast medium are performed, see Fig. 3. A sensitivity study involving numerous tests leads to the relation between the decrease of the maximum measured strain gauge values at the weld toe, the optically evaluated surface crack, and to the corresponding crack depth based on micrographs of the pre-fatigued specimens. In Fig. 3a, a drop of about *20 %* of the initial stress $\sigma_{max,1}$ down to $\sigma_{max,2}$ is observed. The attendant optical evaluation of the surface crack behaviour for the two corresponding fatigue lives in Fig. 3b shows a technical crack initiation at *N=7e4* and $\sigma_{max,2}$ at which the fatigue testing is afterwards stopped.

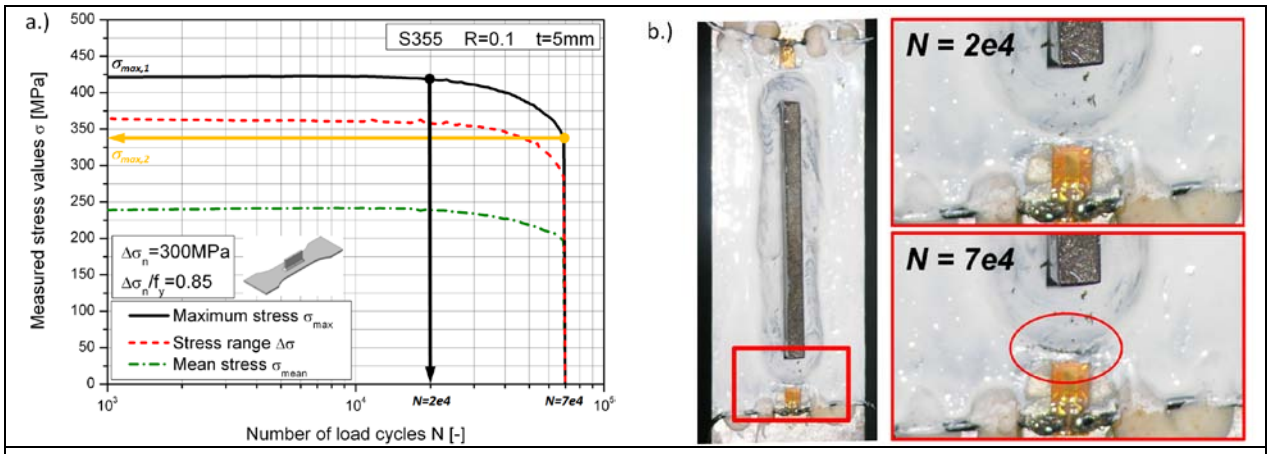

Figure 3: a.) Strain gauge measurements and b.) Optical surface crack detection [9]

Based on the presented experimental procedure a pre-cycling of the specimens in the as-welded condition up to a defined crack depth is enabled, see also [10]. In Fig. 4 the resulting pre-fatigued S/N-curve implying a crack depth of about *a=1mm* in comparison to the previously depicted tests up to burst fracture is evaluated by a survival probability of P_S=*50 %*. Thereby, only a minor difference is noticeable, which is caused by the fact that the bulk of the total lifetime is spent in the small crack size region. Experimental and numerical investigations in [11] show that about *80 %* of the total fatigue life is spent up to *20 %* of the related wall thickness, which basically proof the results in this paper. The pre-fatigued specimens are further on used to assess the potential of the HFMI-treatment as rehabilitation method.

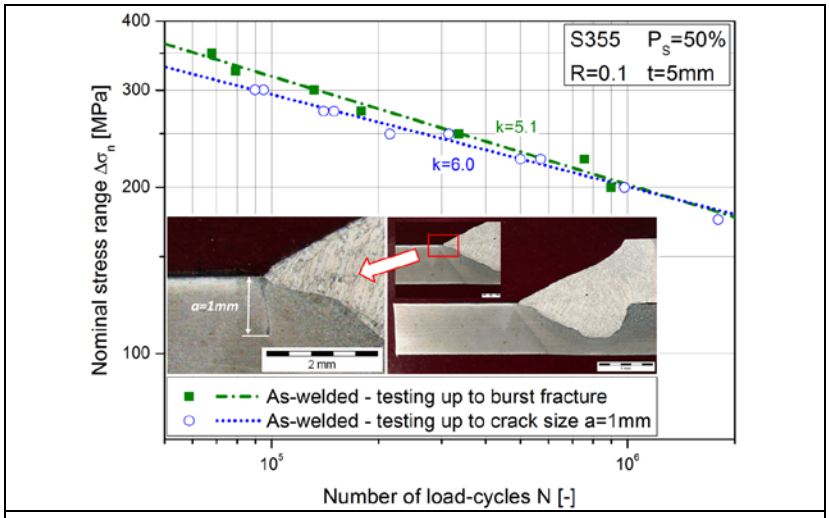

Figure 4: Comparison of test results with specimens up to burst fracture and crack size *a=1mm*

3 Local stress condition

For the evaluation of the local notch stress distribution in depth at the weld toe, a quarter-symmetric model with a hexahedral element mesh and a unified tension load is set-up. The modelled geometry depicts the technical cross-section of the specimens and local deviations from the design geometry are not incorporated in detail. As distortion measurements of the specimens before fatigue testing exhibit only minor values up to one degree angular deformation, a consideration in the numerical analysis is not necessary [1]. The mesh is built-up in accordance to the recommended values for the effective notch stress assessment in [12], and is adapted for each analysed weld toe radius. The stress evaluation is performed for the component *S11* appearing in loading direction of the specimen and therefore most significant for the subsequent crack propagation analysis, see Fig. 5a.

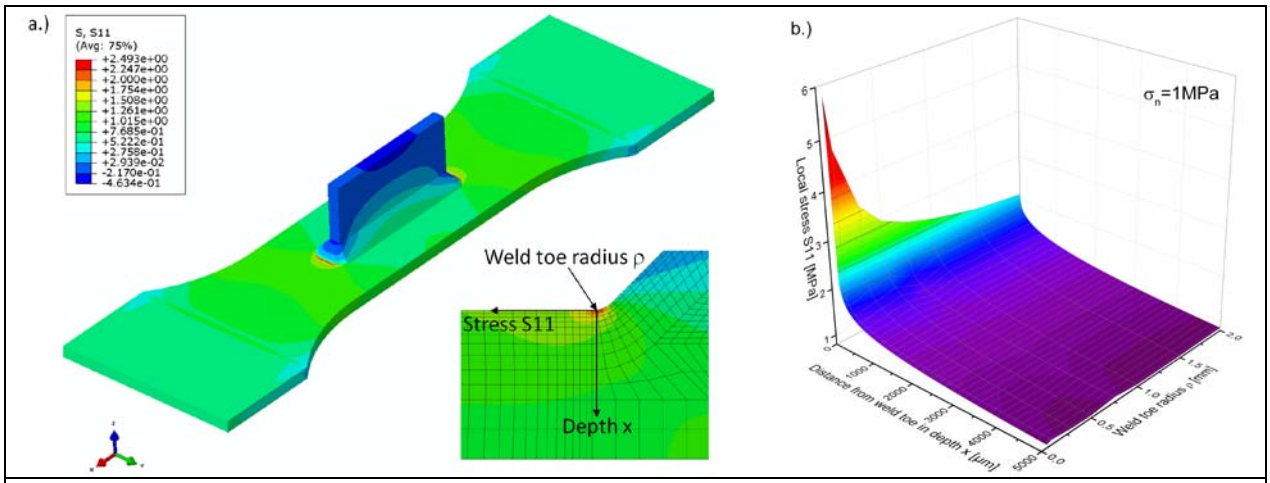

Figure 5: a.) Numerical model for analysis of local stress condition and b.) In-depth notch stress distribution in dependency of weld toe radius

In Fig. 5b the results of the numerical stress analysis is depicted. Thereby, the local stress distribution in depth in dependency of the weld toe radius, ranging from ρ*=0.05* to *2 mm*, is presented. It is shown that at the surface region up to a depth of about *0.1 mm* the weld toe radius has a major influence on the local stress condition. Especially for small radii of about ρ*=0.05* up to *0.2 mm* a high stress concentration is evaluated.

4 Structural weld simulation

In order to improve the accuracy of the crack propagation results also the residual stress condition needs to be incorporated. In general, residual stresses can be determined by means of measurements or numerical analysis. Basic investigations involving a structural weld simulation of the investigated joint type and material are shown in [13]. Thereby, an enhanced method to incorporate the transient work-hardening effect of different material phases into a thermo-mechanically coupled structural weld process simulation is presented, whereat the work-hardening behaviour of metals principally differs for soft ferritic-perlitc and hard bainitic, or even martensitic, phases. For the conducted thermo-mechanical coupled weld process simulation the software package Sysweld [14] is utilized, which supports the implementation of different work-hardening models, such as the basic isotropic behaviour and the kinematic hardening rule according to [15]. Moreover, it is possible to apply the kinematic portion [16], which takes, beside the effect of backstress, the influence of dynamic recovery during cyclic loading into account [17].
One of the main drawbacks of the described material models is, that they are basically not able to consider the effect of phase-change during the transient weld simulation. This means, that the unique material property database is defined at the stage of input card definition and cannot be easily modified for each element possessing process time- and temperature-dependent different hardening parameters, see [13].

To solve the task of transient change in work-hardening per element during the numerical simulation process, a user-defined SIL-routine was previously developed [18]. It enables the implementation of a temperature- and phase-dependent work-hardening behaviour during the transient thermo-mechanical weld simulation. Based on low-cycle-fatigue test results, three different work-hardening behaviours are classified, which depend on the temperature and the major phase content, separated in mainly ferritic-perlitc as soft microstructure; predominantly bainitc-martensitic as hard phase or mixed microstructure. At ambient temperature, the kinematic behaviour is more appropriate, whereas at higher temperatures, close to the austenitic region, the isotropic work-hardening rule is more applicable. The results of the mixed material model calculate the residual stress condition quite well [13]. These results are applied for the investigations in this paper. In Fig. 6a the conducted structural weld simulation model and the temperature distribution during welding is displayed.

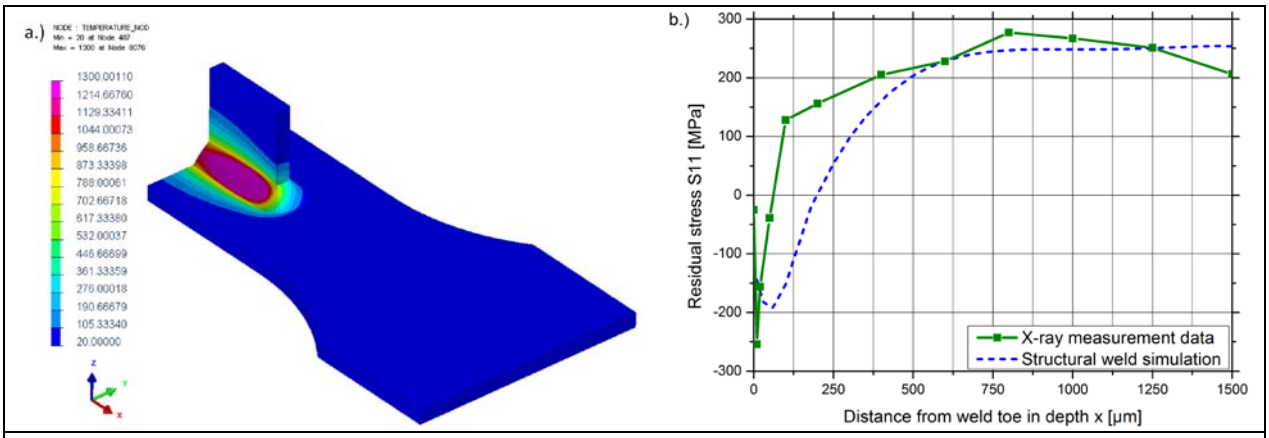

Figure 6: a.) Temparature distribution during welding and b.) Comparison of measured and simulated residual stress values

In Fig. 6b the numerically evaluated residual stress values *S11* in depth are compared to experimental data by X-ray measurements for the as-welded condition. Additional residual stress measurements in [9] focussing on the base material exhibit a major compressive residual stress state in the surface layer of the metal sheet, which primarily emerge due to the base-material rolling process. By taking these compressive stresses also for the numerical weld simulation into account, the results in the as-welded condition show a good compliance to the measured values and are therefore used for the subsequent crack propagation analysis.

5 Crack propagation analysis

Fracture mechanical approaches provide the basis for the assessment of cracks or crack-like imperfections, where the crack propagation significantly exceeds the crack initiation phase, see [19]. For welded joints, the basic elements of the linear-elastic crack growth calculation are the stress intensity factor *K*, the crack shape and path and the chosen material parameters, see Tab. 1. The crack propagation is mostly calculated based on the simple power law according to Paris and Erdogan [20]:

$$\frac{da}{dN} = C \cdot \Delta K^{m} \quad \text{for} \quad \Delta K > \Delta K_{th} \qquad \text{Equ. 1}$$

For simple crack geometries and load configurations numerous stress intensity factor formulae are available [21]. However, there are basically no ready-made solutions for welded structures except for a few crack configurations. Therefore, the weight function technique [22, 23] was employed in order to determine stress intensity factors for cracks in real welded structures, see [24].

Table 1: Recommended crack propagation data for steel [25]

Paris power law parameters (charact. values)	**Threshold values ΔK_{th} [MPa$\sqrt{m}$]**			
	R > 0.5	***0 ≤ R ≤ 0.5***	***R < 0***	***Surface crack depth < 1mm***
$C=9.5 \cdot 10^{-12}$ m=3.0	*2.0*	*5.4 – 6.8·R*	*5.4*	*≤ 2.0*

5.1 Weight-function approach

The weight function approach is basically defined as the stress intensity factor *K* induced by the simplest load configuration, such as a pair of unit forces *F* attached to the crack surface, see Fig. 7. The operation of each differential force on a crack is specified by the weight-function. [24, 25]

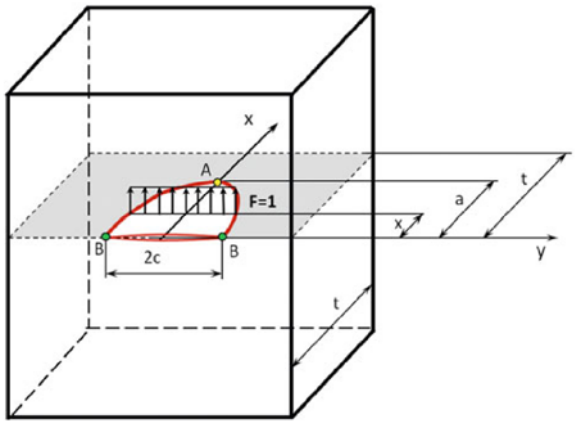

Figure 7: Semi-elliptical surface crack in plate [26]

A general form to describe the weight function is provided by [23] according to Equ. 2. The containing parameters M_1, M_2 and M_3 are in dependency of the actual crack geometry and listed in [23, 24] for numerous crack configurations. For the crack propagation analysis of the investigated longitudinal stiffener in this paper, the accordant expressions for a semi-elliptical crack at the deepest point A are applied.

$$m(x,a)=\frac{2\cdot F}{\sqrt{2\cdot\pi\cdot(a-x)}}\cdot\left[1+M_1\cdot\left(1-\frac{x}{a}\right)^{\frac{1}{2}}+M_2\cdot\left(1-\frac{x}{a}\right)+M_3\cdot\left(1-\frac{x}{a}\right)^{\frac{3}{2}}\right] \qquad \text{Equ. 2}$$

To calculate the stress intensity factor *K* the knowledge of the stress distribution $\sigma(x)$ in the prospective crack plane of the un-cracked plate is required. In [25] it is recommended to involve the stress distribution assuming a weld toe radius of $\rho=0$ to 0.2 *mm*, which is already computed within the local stress analysis depicted in chapter three.Further on, the stress intensity factor *K* is calculated by integrating the product of the stress distribution $\sigma(x)$ and the weight function $m(x,a)$ for each crack increment during cyclic loading, see Equ. 3.

$$K=\int_0^a \sigma(x)\cdot m(x,a)\cdot dx \qquad \text{Equ. 3}$$

To calculate the fatigue life more precisely the influence of the residual stress condition at the vicinity of the crack at the weld toe has to be considered. Based on the numerically evaluated residual stress condition, a procedure based on investigations in [27] involving an effective stress ratio R_{eff} [28] at the crack tip, is applied, see Equ. 4.

$$\frac{da}{dN}=C\cdot\left(\frac{\Delta K}{1.5-R_{eff}}\right)^m \qquad \text{Equ. 4}$$

The stress intensity factor range ΔK is defined by the difference of the maximum and minimum stress intensity factor at the crack tip and is not affected by the residual stress state, see Equ. 5.

$$\Delta K=K_{\max}-K_{\min} \quad \text{with} \quad K_{\max/\min}=\int_0^a \sigma_{\max/\min}(x)\cdot m(x,a)\cdot dx \qquad \text{Equ. 5}$$

In accordance to the loading dependent stress intensity factors K_{max} and K_{min}, the residual stress intensity factor K_{res} is calculated in the same way, see Equ. 6. The residual stress distribution in depth $\sigma_{res}(x)$ is derived from the result of the structural weld simulation.

$$K_{res} = \int_0^a \sigma_{res}(x) \cdot m(x,a) \cdot dx \qquad \text{Equ. 6}$$

Finally, the effective stress ratio R_{eff} is defined as shown in Equ. 7. Thereby, the local stress ratio at the crack tip is influenced by the local residual stress condition and in this way incorporated in the crack propagation analysis and fatigue life assessment.

$$R_{eff} = \frac{K_{\min} + K_{res}}{K_{\max} + K_{res}} \qquad \text{Equ. 7}$$

Fracture mechanical calculations are performed in accordance to the presented procedure for the longitudinal stiffener specimen. For the crack shape, the aspect ratio *a/c* is one important influence factor, whereat general applicable recommendations are provided in [25]. As a conservative approach a ratio of *a/c=0.1* may be defined, but the calculation results exhibited that the computed lifetime is significantly lower than the fatigue test results. Therefore, the proposed formula for ends of longitudinal stiffeners in [25] is applied (Equ. 8), leading to a/c-values of *0.7* to *0.8*, which are also in good accordance to the test results of the fractured specimens.

$$c = \frac{6.71 + 2.58 \cdot a}{2} \qquad \text{Equ. 8}$$

A comparison of the calculated N_{calc} and experimentally evaluated load-cycles N_{exp} is presented in Fig. 8 as normalized ratio N_{calc} / N_{exp} in dependency of the initial crack length a_i and the weld toe radius ρ. Basically, it is shown that initial crack length value of a_i*=0.1 mm* is generally well applicable, but also values of a_i*=0.05 mm* which are suggested for mechanical engineering applications or a_i*=0.15 mm* as a conservative approach by fitness for purpose codes [25] are acceptable. However, to analyse the influence of the initial crack length in detail, a variation of a_i*=0.05* up to a_i*=0.2 mm* is included. In the finite lifetime regime at a nominal stress ratio of $\Delta\sigma_n$*=200MPa* the calculated load-cycles are affected by the weld toe radius only in case of minor initial crack lengths of a_i*=0.05 mm*, leading to a significant overestimation of the lifetime, see Fig. 8a. For higher initial crack values, the influence of the weld toe radius is consequently decreasing.
On contrary, in the high-cycle fatigue region at a nominal stress ratio of $\Delta\sigma_n$*=100MPa* the minimum investigated initial crack length tend to result in a good accordance to the fatigue tests incorporating weld toe radii smaller than ρ*=0.2 mm*, see Fig. 8b. Assuming a higher notch radius, the calculated lifetime is overestimated up to a factor of eight and is therefore, not applicable. Summarized, the calculated lifetime N_{calc} is strongly influenced by the weld toe radius, especially at a minor defined initial crack length of about a_i*=0.05 mm*.

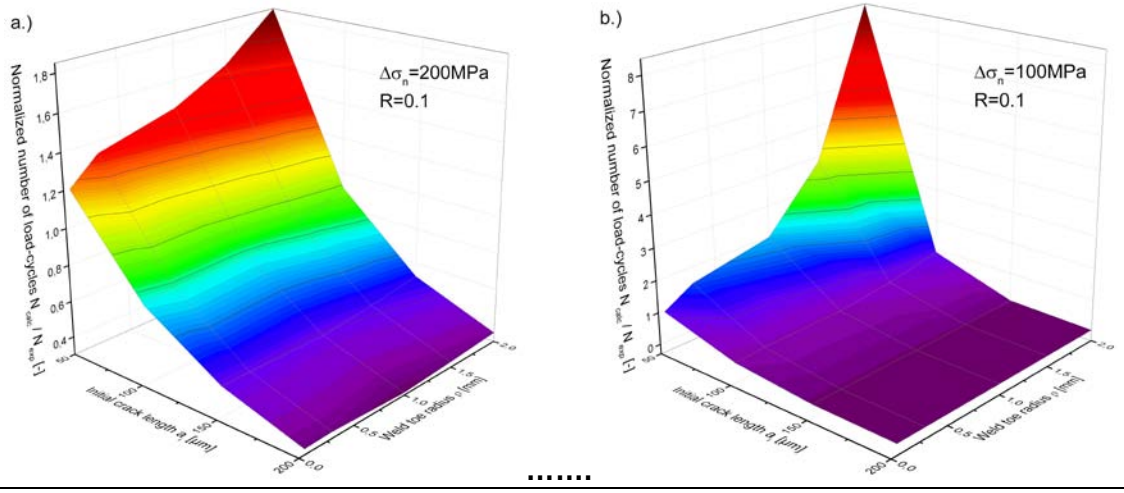

Figure 8: Normalized number of load-cycles N_{calc} / N_{exp} at a nominal stress range of a.) $\Delta\sigma_n$=200MPa and b.) $\Delta\sigma_n$=100MPa

As the calculated lifetime is significantly affected by the initial crack length and the weld toe radius at the high-cycle fatigue region, a detailed analysis for the load-level involving a nominal stress of $\Delta\sigma_n$=*100MPa* is performed, see Fig. 9. Thereby, the influence of the weld toe radius on the stress intensity factor range ΔK in dependency of the actual crack length *a* is quite small, see Fig. 9a. Especially if the crack is enough propagated and not influenced by the stress concentration at the weld toe region anymore, the impact of the weld toe radius and the associated stress distribution on the stress intensity factor is negligible. Fig. 9b displays the stress intensity factor range ΔK related to the minimum recommended [25] threshold value of $\Delta K_{th,min}$=*2 MPa*$\sqrt{m}$ in dependence of the initial crack length a_i and the weld toe radius ρ. One can see, that especially for minor values of a_i<*0.1 mm* the actual ΔK is below the threshold value and therefore, basically no crack propagation occurs.

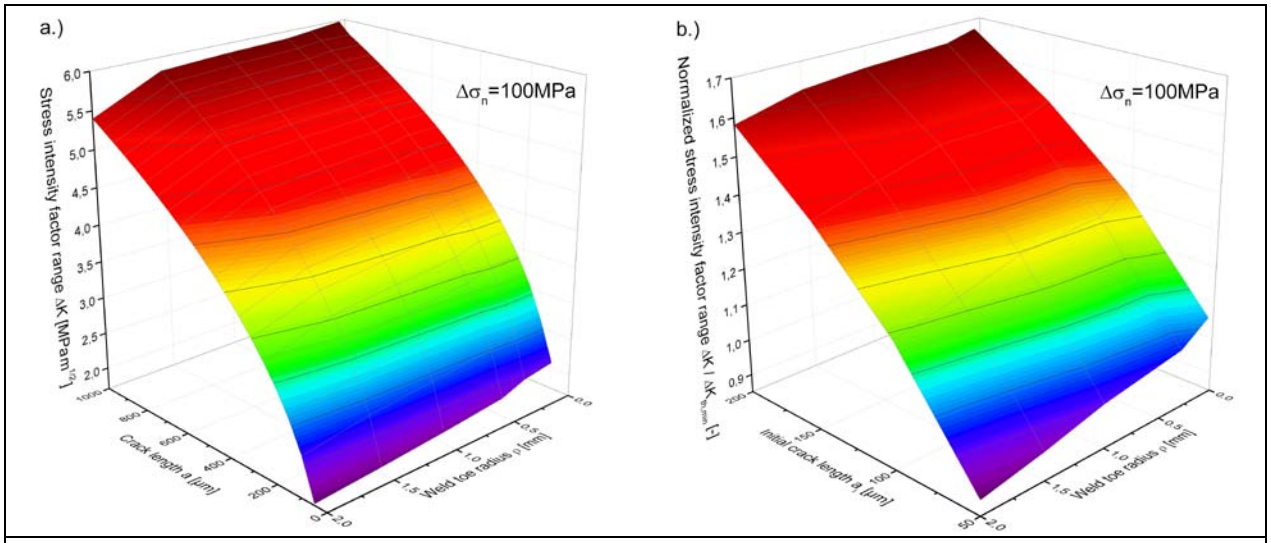

Figure 9: a.) Stress intensity factor range ΔK during crack propagation and b.) Ratio of ΔK / $\Delta K_{th,min}$ in dependency of initial crack length a_i

Summarized, an initial crack length of a_i=*0.1 mm* and a weld toe radius of ρ=*0.05 mm* leads to a good accordance to the fatigue test results and are also in agreement to the recommended values [25]. These values are further on applied for the successive crack propagation analysis.

Fig. 10a shows the effective stress ratio R_{eff} at the crack tip in dependence of the stress ratio *R* due to the loading and the actual crack length *a*. As the influence of the residual stress condition is considered by R_{eff}, the effect of the residual stress distribution is clearly observable for the lowest stress ratio of *R*=*-1*. In this case, the compressive residual stress state at the surface layer of the weld toe region affects the local stress ratio R_{eff} in a major way. If the crack propagates, the effect is reduced and at a crack depth of about *a*=*0.5 mm* no more influence is observable.

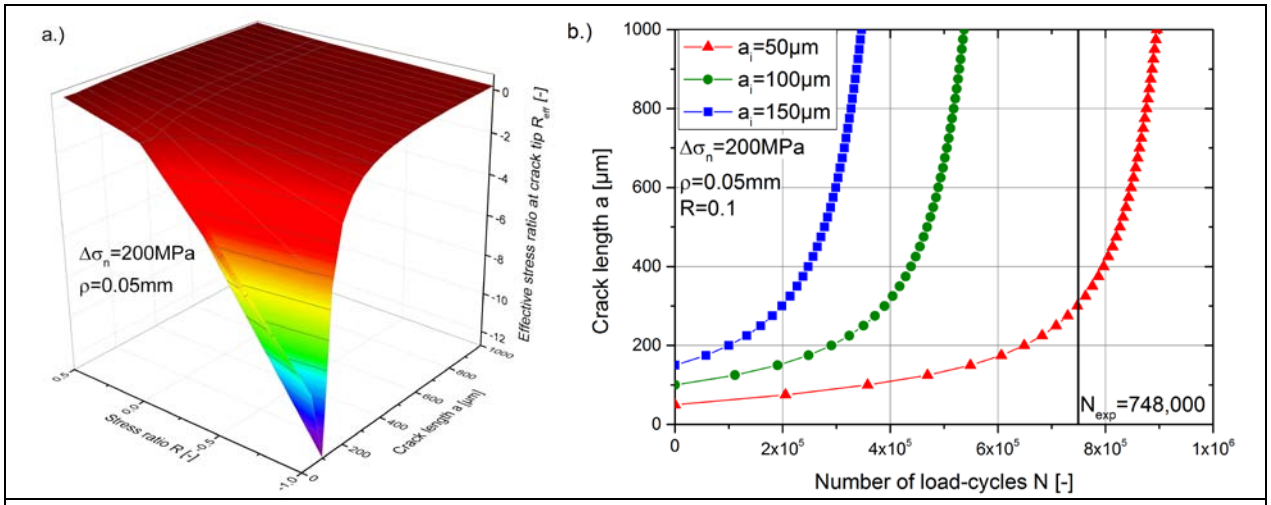

Figure 10: a.) Effective stress ratio R_{eff} at crack tip and b.) Calculated a/N-curves for different initial crack lengths a_i

On contrary, for high applied tumescent load-ratios of *R=0.5* there is almost no effect of the residual stress condition on the local stress ratio at the crack tip. This validates the IIW-recommendation, whereat a fatigue testing at high mean stresses, preferably at *R=0.5* should be conducted in order to minimize the influence of the weld process induced residual stress condition.
In Fig. 10b the resulting a/N-curves for a nominal stress range of $\Delta\sigma_n$*=200MPa* and the applied stress ratio of *R=0.1* is depicted for different initial crack lengths a_i. As already stated, an assumption of a_i*=0.05 mm* may lead to an overestimation of the lifetime, which is also evaluated in this case. The recommended value of a_i*=0.1 mm* calculates the lifetime in a safe but appropriate way, and further on, a definition of a_i*=0.15 mm* leads, as expected, to a conservative fatigue life assessment.

5.2 Parametric equation approach

In case of simple weld geometries, such as butt welds, T-joints or longitudinal stiffeners, parametric formulae are provided [25, 29]. Thereby, the stress intensity factor *K* is calculated according to Equ. 9 considering the crack-geometry dependent correction function *Y(a)* and an additional adjustment for the local notch of the weld toe $M_k(a)$. In [30] the magnification factor M_k is presented, leading to a comparable condition for a crack of the same geometry, but without the presence of the weld. Furthermore, a separation of membrane σ_m and shell bending stress σ_b is necessary for most of the parametric formulae, whereat the resulting stress intensity factor *K* is computed as a superposition of both stress components.

$$K = \sqrt{\pi \cdot a} \cdot \left[\sigma_m \cdot Y_m(a) \cdot M_{k,m}(a) + \sigma_b \cdot Y_b(a) \cdot M_{k,b}(a)\right] \qquad \text{Equ. 9}$$

In [25] the stress magnification factor M_k for the end-of-seam region of a longitudinal stiffener is defined based on Equ. 10. Herein, the factor *C* and exponent *k* depend on the dimensions of the corresponding weld detail.

$$M_k = C \cdot \left(\frac{a}{t}\right)^k \qquad \text{Equ. 10}$$

Recent studies [31] involving a comparison of analytical, numerical and experimental results show a good accordance and the basic applicability of the presented parametric formulae.

5.3 Comparison of results

To validate the fracture mechanical calculation, the calculated lifetime values are compared to the experimental fatigue test results, see Tab. 2. Thereby, the initial crack length is set to the recommended value of a_i*=0.1 mm* and the calculations are performed up to a final crack length of a_f*=1 mm*, because as shown in Fig. 4, within this crack propagation region most of the lifetime is spent and just a minor remaining lifetime up to burst fracture is evaluated.

Table 2: Evaluated lifetime *N* for different load-levels

Initial crack length a_i=0.1mm				
Nominal stress range $\Delta\sigma_n$ [MPa]	N_{exp} [-]	N_{WF} [-] (incl. RS)	N_{WF} [-] (excl. RS)	N_{PE} [-] (excl. RS)
100	*2.1e7*	*1.5e7*	*1.3e6*	*194,000*
200	*748,000*	*537,000*	*164,000*	*24,000*
300	*95,000*	*100,000*	*48,000*	*7,000*

Firstly, a comparison of the experimental lifetime N_{exp} and the calculated load-cycles by the weight-function approach N_{WF} show, that by including the residual stress (RS) condition a well-matching fatigue assessment is possible. On contrary, the exlusion of the residual stress state leads to a significant reduction of the calculated lifetime, which can be explained by the mainly compressive residual stresses at the surface region maintaining a reduced crack propagation rate and therefore, an increased lifetime. The effect of the residual stress field on the crack propagation of surface cracks is principally analysed in [32].
Secondly, the application of the parametric equation approach to assess the fatigue life exhibits the lowest and most conservative lifetime values N_{PE}. Also in this case, the beneficial compressive residual stresses are not considered, conducting to a major decrease for the lifetime estimation. However, one advantage of this method is the simple applicability with less effort and expenditure of time.

6 Rehabilitation of pre-fatigued structures

6.1 Methods

If a crack is detected or the service time of the structure or component is completed, several rehabilitation methods are applicable. Simple retrofitting techniques are to attach bolted splices to the cracked parts or to achieve crack-growth arrest by drilling sop holes at the end of cracks [33]. A more elaborated way to restore cracked areas is fulfilled by re-welding. Especially wear damaged sections of supporting structures are often weld-repaired, whereat an influence by the tri- or bi-metal system on the fatigue crack growth should be analysed [34]. Another weld-repair technique which also improves the fatigue performance is based on the application of low temperature transformation welding wires. Thereby, compressive residual stress fields in the vicinity of the weld bead are introduced which has a beneficial effect on crack initiation and propagation and therefore enhances the fatigue strength [35].
Further technologies to rehabilitate pre-fatigued structures are by the application of post-treatment methods. In [36], tungsten inert gas (TIG) and plasma dressing are applied to repair crack-containing T-welded joints. It is shown that by TIG-dressing only crack depths up to *2.5 mm* can be successfully repaired. By the aid of plasma dressing the results show an effect also for greater crack depths up to *4 mm*, whereat the fatigue lives were found to be similar as for the as-welded condition. An overview of further available repair methods like the local explosive treatment, local heat treatment, and high-frequency mechanical impact (HFMI) treatment with traditional techniques is given in [37]. However, based on the applicability and industrial feasibility the HFMI-treatment is one utmost efficient method, which is further on exemplified.

6.2 HFMI-treatment

Not only for un-cracked, but also for pre-fatigued joints recent investigations [10, 38, 39] show a great beneficial effect for rehabilitation by the HFMI-treatment, whereat the fatigue strength of the repaired specimens is equal or even exceeds the HFMI-treated condition without pre-cycling. As described, pre-fatigued specimens with a crack length of *a=1 mm* are analysed to assess the potential of HFMI as rehabilitation method without additional re-welding. A comparison of the evaluated fatigue test results are shown in Fig. 11. Thereby, the fatigue enhancement by the rehabilitation in the finite lifetime regime basically increases with a decreasing nominal load stress range. In the high-cycle fatigue region, the fatigue strength at the run-out level is almost identical to the HFMI-treated curve without pre-fatigue.

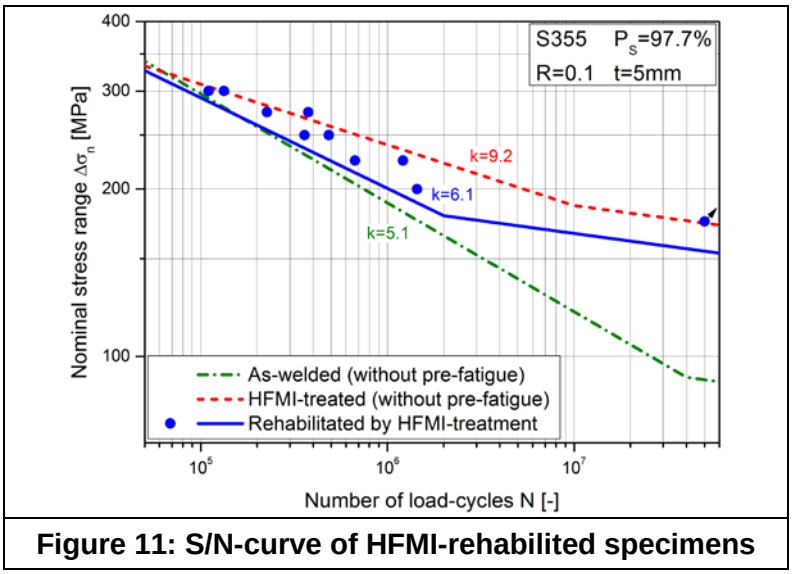

Figure 11: S/N-curve of HFMI-rehabilited specimens

The results are in good agreement with the previous investigations in literature, which generally confirm the applicability of the HFMI-treatment as rehabilitation technique. One main influencing factor on the effectiveness is the crack length before performing the HFMI-rehabilitation. In [10] it is shown, that for crack lengths above one to two millimetres a significant reduction of the benefit occurs, which can be explained by the limited penetration depth by the HFMI-treatment, depending on the local notch geometry, material properties, and post-treatment parameters.

For the quantification of the rehabilitation benefit by the mechanical post-treatment a beneficial gain factor g_N is introduced in [10]. The value is defined as the ratio of the fatigue life of the repaired joint N_r to the expected fatigue life of the joint it if was not repaired N_e, see Equ. 11 and Equ. 12.

$$N_r = N_i + N_{bh} + N_{aH} \quad \text{Equ. 11}$$

$$N_e = N_i + N_{bh} + N'_{aH} \quad \text{Equ. 12}$$

Thereby, N_i is the crack initiation life before the first crack for repair starts, N_{bh} is the fatigue life in crack propagation, N_{aH} is the fatigue life after repair including crack initiation and propagation stage, and N'_{aH} is the fatigue life that would be obtained if the HFMI-repair-treatment would not be performed. A calculation of the gain factor g_N for the investigated test series indicates that the beneficial effect for a constant pre-crack length is depending on the applied load level, whereat for a higher nominal stress at $\Delta\sigma_n$*=300MPa* the assessment leads to g_N*=1.01* and for a lower nominal stress at $\Delta\sigma_n$*=200MPa* to g_N*=1.60.* The evaluated values are basically in good accordance to the results presented in [10]. Especially for complex welded structures an exactly measurement of the crack length is not always possible leading to an uncertainty of the applicability by the HFMI-treatment. In this case, a re-welding and additional HFMI-post treatment as rehabilitation procedure is recommended, see [40].

7 Conclusion

Crack propagation analysis of the investigated longitudinal stiffener based on the application of the weight-function approach and considering the local residual stress condition leads to a good agreement with the evaluated fatigue test results. On contrary, by neglecting the residual stress state the deviation significantly increases towards a conservative design, due to an essential change of the local effective stress ratio R_{eff} at the crack tip during propagation in case of the analysed load-applied stress ratio of *R=0.1*. Additional numerical studies show a great influence of the weld toe radius, whereat an applied value of ρ*=0.05 mm* exhibits appropriate results of the fracture mechanical calculations and matches well with the recommendation. A final comparison to the fracture mechanical standard approach based on parametric formulae shows that this method leads to a conservative assessment of the fatigue life.
Fatigue test results in as-welded, HFMI-treated, and pre-cycled up to a crack length of *a=1 mm* and subsequent HFMI-repair indicate a beneficial effect of the mechanical post-treatment as post-treatment for pre-cracked joints. The fatigue strength after rehabilitation generally depends on the crack length before repair and furthermore on the applied load level, whereat the benefit increases with a decrease of the nominal stress range. Based on the investigations and results within this work and by consideration of previously analyses regarding fatigue crack growth assessment and rehabilitation of pre-fatigued structures, the following conclusions can be drawn:

- The weight-function approach including an incorporation of the local residual stress condition is well applicable to assess the crack growth of welded joints based on the recommended values with a weld toe radius of ρ*=0.05 mm* and an initial crack size of a_i*=0.1 mm*.
- An estimation of the crack size based on parametric formulae to calculate the stress intensity factor range ΔK and stress magnification factor M_k usually leads to a conservative assessment and underrating of the lifetime up to a defined final crack length.
- On the basis of the results within this work it can be concluded that if a structure is pre-fatigued and a certain crack size is detected, the remaining service life can be accurately and efficiently assessed based on the fracture mechanical weight-function approach.
- For a rehabilitation of pre-fatigued structures, the applied method significantly depends on the actual crack size. In general, a rehabilitation procedure involving grinding, re-welding and a final additional post-weld treatment is recommended. However, due to a limited time and cost frame, this elaborated routine cannot be completely fulfilled in industrial applications in some cases.
- If the HFMI-treatment is applied without previous grinding and re-welding of the weld toe, a maximum crack size in depth of about *a=0.5 mm* acts as conservative proposal for mild steel joints. For an application up to this value the rehabilitation should lead to an enhancement of the fatigue life in the finite-lifetime and high-cycle fatigue region. Due to different forming capacities and work-hardening potentials the applicability of this maximum crack size value cannot be guaranteed for high-strength steel joints and needs to be investigated specifically.

REFERENCES

[1] Hobbacher A.: IIW Recommendations for Fatigue Design of Welded Joints and Components, WRC Bulletin 520, The Welding Research Council, New York, 2009.

[2] Hobbacher A.: The use of fracture mechanics in the fatigue analysis of welded joints, Fracture and Fatigue of Welded Joints and Structures, pp. 91-112, 2011.

[3] Zerbst U., Ainsworth R.A., Beier H.Th., Pisarski H., Zhang Z.L., Nikbin K., Nitschke-Pagel T., Münstermann S., Kucharczyk P., Klingbeil D.: Review on fracture and crack propagation in weldments – A fracture mechanics perspective, Engineering Fracture Mechanics, vol. 132, pp. 200-276, 2014.

[4] Ditchburn R.J., Burke S.K., Scala C.M.: NDT of welds: state of the art, NDT&E International, vol. 29, pp. 111-117, 1996.

[5] Yildirim H.C., Marquis G.B.: Overview of fatigue data for high frequency mechanical impact treated welded joints, Welding in the World, vol. 56, no. 7/8, pp. 82-96, 2012.

[6] Leitner M., Stoschka M., Eichlseder W.: Fatigue enhancement of thin-walled, high-strength steel joints by high-frequency mechanical impact treatment, Welding in the World, vol. 58, pp. 29-39, 2014.

[7] Marquis G.B., Mikkola E., Yildirim H.C., Barsoum Z.: Fatigue strength improvement of steel structures by high-frequency mechanical impact: proposed fatigue assessment guidelines, Welding in the World, vol. 57, pp. 803-822, 2013.

[8] Marquis G.B., Barsoum Z.: Fatigue strength improvement of steel structures by high-frequency mechanical impact: proposed procedures and quality assurance guidelines, Welding in the World, vol. 58, pp. 19-28, 2014.

[9] Leitner M.: Local fatigue assessment of welded and high frequency mechanical impact treated joints, PhD-thesis, Montanuniversität Leoben, 2013.

[10] Branco C.M., Infante V., Baptista R.: Fatigue behaviour of welded joints with cracks, repaired by hammer peening, Fatigue Fract Engng Mater Struct, vol. 27, pp. 785-798, 2004.

[11] Shah F.: Crack propagation analysis of welded joints by numerical and experimental investigations, Master thesis, Montanuniversität Leoben, 2015.

[12] Fricke W.: Guideline for the Fatigue Assessment by Notch Stress Analysis for Welded Structures, IIW-Document XIII-2240r1-08/XV-1289r1-08, 2008.

[13] Stoschka M., Ottersböck M.J., Leitner M.: Integration of Phase-Dependent Work-Hardening into Transient Weld Simulation, Proceedings of the Ninth International Conference on Engineering Computational Technology, Paper 39, 2014.

[14] ESI Group: SYSWELD Toolbox, release 16, 2014.

[15] Prager W.: Recent development in the mathematical theory of plasticity, Journal of Applied Physics, vol. 235, issue 7, 1949.

[16] Armstrong P., Frederick C.: A mathematical representation of the multiaxial bauschinger effect, CEGB Report RD/B/N731, 1966.

[17] Chaboche J.-L.: A review of some plasticity and viscoplasticity constitutive theories, International Journal of Plasticity, vol. 24, pp. 1642-1693, 2008.

[18] Ottersböck M., Stoschka M., Thaler M.: Study of kinematic strain hardening law in transient welding simulation, Mathematical Modelling of Weld Phenomena, vol. 10, pp. 255-266, 2013.

[19] Fricke W.: Fatigue analysis of welded joints: state of development, Marine Structures, vol. 16, pp. 185-200, 2003.

[20] Paris P., Erdogan F.: A critical analysis of crack propagation laws, Journal of Basic Engineering, Transactions of the American Society of Mechanical Engineers, vol. 85, no. 4, pp.528-534, 1963.

[21] Murakami Y.: Stress intensity factors handbook, Pergamon Press, Oxford, vol. 2, 1987.

[22] Bueckner H.F.: A novel principle for the computation of stress intensity factors, Zeitschrift fur Angewandte Mathematik und Mechanik, vol. 50, pp. 529-546, 1970.

[23] Glinka G., Shen G.: Universal features of weight functions for cracks in Mode I, Engineering Fracture Mechanics, vol. 40, no. 6, pp. 1135-1146, 1991.

[24] Chattopadhyay A., Glinka G., El-Zein M., Qian J., Formas R.: Stress analysis and fatigue of welded structures, Welding in the World, vol. 55, no. 7/8, pp. 2-21, 2011.

[25] Hobbacher A.: Update of the Fracture Mechanics Chapters of the IIW Fatigue Design Recommendations, IIW-document XIII-2370r1-11 / XV-1376r1-11, 2012.

[26] Goyal R., Glinka G.: Fracture mechanics-based estimation of fatigue lives of welded joints, Welding in the World, vol. 57, pp. 625-634, 2013.

[27] Glinka G.: Effect of residual stresses on fatigue crack growth in steel weldments under constant and variable amplitude loading, Fracture Mechanics, ASTM STP 677, American Society for Testing and Materials, pp. 198-214, 1979.

[28] Kurihara M., Katoh A., Kwaahara M.: Analysis on fatigue crack growth rates under a wide range of stress ratio, Journal of Pressure Vessel Technology, Transactions of the ASME, vol. 108, no. 2, pp. 209-213, 1986.
[29] Hobbacher A.: Stress intensity factors of welded joints, Engineering Fracture Mechanics, vol. 46, no. 2, pp. 173-182, 1993 and vol. 49, no. 2, p. 323, 1994.
[30] Maddox S.J.: An analysis of fatigue cracks in fillet welded joints, International Journal of Fracture, vol. 11, no. 2, pp. 221-243, 1975.
[31] Al-Mukhtar A.M., Henkel S., Biermann H., Hübner P.: A Finite Element Calculation of Stress Intensity Factors of Cruciform and Butt Welded Joints for Some Geometrical Parameters, Jordan Journal of Mechanical and Industrial Engineering, vol. 3, no. 4, pp. 236-245, 2009.
[32] Mochizuki M., Miyazaki K.: Surface crack propagation analysis under residual stress field, Welding in the World, vol. 50, no. 5/6, pp. 38-45, 2006.
[33] Miki C.: Retrofitting Engineering for Fatigue Damaged Steel Structures, IIW-document XIII-2284-09 / WG5-74-07, revised 2008.
[34] Zhang C., van der Vyver S., Hua X., Lu P.: Fatigue crack growth behavior in weld-repaired high-strength low-alloy steel, Engineering Fracture Mechanics, vol. 78, pp. 1862-1875, 2011.
[35] Miki C., Hanji T., Tokunaga K.: Weld repair for fatigue-cracked joints in steel bridges by applying low temperature transformation welding wire, Welding in the World, vol. 56, no. 3/4, pp. 40-50, 2012.
[36] Ramalho A., Ferreira J., Branco C.: Fatigue behaviour of T welded joints rehabilitated by tungsten inert gas and plasma dressing, Materials and Design, vol. 32, pp. 4705-4713, 2011.
[37] Kudryavtsev Y., Kleiman J., Knysh V., Mikheev P.: Fatigue Life Improvement of Structural Elements with Fatigue Cracks, Proceedings of the SEM Annual Conference & Exposition on Experimental and Applied Mechanics, 2002.
[38] Kudryavtsev Y., Kleiman J., Lobanov L., Knysh V., Voitenko O., Prokopenko G., Lugovskoy A.: Rehabilitation and repair of welded elements and structures by ultrasonic peening, Welding in the World, vol. 51, no. 7/8, pp. 47-43, 2007.
[39] Weich I.: Ermüdungsverhalten mechanisch nachbehandelter Schweißverbindungen in Abhängigkeit des Randschichtzustands, PhD-thesis, Technische Universität Braunschweig, 2009.
[40] Tominaga T., Matsuoka K., Sato Y., Suzuki T.: Fatigue improvement of weld repaired crane runway girder by ultrasonic impact treatment, Welding in the World, vol. 52, no. 11/12, pp. 50-62. 2008.